Renewable Energy 153 (2020) 711–724

Contents lists available at ScienceDirect

Renewable Energy

journal homepage: www.elsevier.com/locate/renene

Torrefaction of woody biomass (*Acacia nilotica*): Investigation of fuel and flow properties to study its suitability as a good quality solid fuel

Satyansh Singh , Jyoti Prasad Chakraborty *, Monoj Kumar Mondal

Department of Chemical Engineering and Technology, Indian Institute of Technology (Banaras Hindu University), Varanasi, 221 005, India

ARTICLE INFO

Article history:
Received 12 June 2019
Received in revised form
9 January 2020
Accepted 10 February 2020
Available online 12 February 2020

Keywords:
Torrefaction
ICP-MS
Contact angle
Angle of repose
Fuel and flow properties
Acacia nilotica

ABSTRACT

Torrefaction of *Acacia nilotica* was carried out in a quartz fixed-bed reactor. Temperature and residence time varied from 220 to 280 °C and 20–60 min. The fuel (volatile ignitability (VI), combustibility index (CI), fuel ratio (FR)), and flow (Hausner ratio (HR), cohesion coefficient (C), Carr compressibility index (CCI), angle of repose) properties were investigated for raw and torrefied biomass. Torrefied biomass was also characterized through TGA, FTIR, SEM-EDX and ICP-MS analysis. For moisture sorption test, contact angle was measured. Finally, torrefied biomass was compared with coal using published literature. The HHV, fixed carbon content, FR of raw biomass at 280 °C for 40 min was increased from 19.31 to 24.76 MJ/kg, 11.35 to 60.40 wt %, and 0.13 to 1.63, respectively. While, VI, CI, C, CCI and bulk density of raw biomass at similar condition of torrefaction decreased from 15.76 to 15.37 (MJ/kg), 147.40 to 17.37 (MJ/kg), 0.40 to 0.33, 22.85 to 15.86 and 230.82 to 172.84 (kg/m^3), respectively. ICP-MS analysis revealed that torrefied biomass was enriched in sodium, potassium, calcium, magnesium, etc. At similar torrefaction condition, the moisture absorbed by raw and torrefied biomass was 35.44% and 6.61%, respectively. Contact angle (79.1°/77.5°) for torrefied biomass suggested its hydrophobic nature.

1. Introduction

Over the last few decades, the rapid increase in world population, industrialization and high living standard of people, created a huge gap between demand and supply of energy [1]. To fulfill the energy demand, only coal contributes 38% of total electricity generation of the world in 2017 [2]. The reserves of fossil fuel such as coal, petroleum, and natural gas are limited and large exploitation along with complete dependency on the fossil fuel can diminish the fossil fuel reserve. Also, application of fossil fuels severely affects the environment by harmful emission such as SO_x, NO_x, greenhouse gas (CO_2) and particulate matters [3]. The most promising way to solve the problem is to use and extract energy from renewable resources [4].

Though we have wind, solar, geothermal, hydrothermal etc. as renewable energy sources, however, among them biomass is most abundant worldwide and easily available. Various examples of biomass include forest residue, food crops, crops for energy like switch grass or prairie perennials, crop residues like corn stover, wood waste, by-products (both mill residues and traditionally noncommercial biomass in the woods), and animal manure. The consideration of biomass as a carbon-neutral fuel and its quality to emit lesser amount of sulphur and nitrogen makes it important source for the production of bio-energy [5]. *Acacia nilotica*, a kind of forest tree, has vast availability in India, Australia, African, and South East Asian countries [6]. It is a tropical tree having height around 7–18 m and diameter around 20–30 cm [7]. These trees are fast growing, generally found in waste and barren land having low productivity and it does not compete with land application for food production. It is also considered as an important plant having economic value since it is a medicinal plant and good source of tannins and gums [6,8]. In addition, it is a good source of timber wood and used as a fuel and fodder for animals in rural areas in India. *Acacia nilotica* is dispersed all over India along national highways, railway lines, forest areas, roadsides, farmlands, tank foreshores, farm fields, village grazing lands and wastelands. The total wood production from *Acacia nilotica* is 167 tonnes per hectare, while, total pod generation from *Acacia nilotica* is 0.6 million tonnes per year [9–11]. As a fuelwood it is considered as an excellent material as it has high calorific value (~20 MJ/kg) and lesser smoke emission tendency [9]. It is also used in pulp and paper industry and as a fuel in textile and brick kiln [10]. Also, the

* Corresponding author.
E-mail address: jpc.che@iitbhu.ac.in (J.P. Chakraborty).

https://doi.org/10.1016/j.renene.2020.02.037
0960-1481/

charcoal made from *Acacia nilotica* has superior properties from the other biomass species. Different part of *Acacia nilotica* tree (leaf, seed and bark) are used as adsorbent and feedstock for pyrolysis process [12,13].

Regardless of large availability and easy accessibility, biomass is allied with many inherent disadvantages such as high moisture content, non-uniform structure and physical properties such as large volume or low bulk density, low calorific value and hygroscopic nature which hinder the direct application of biomass in thermochemical conversion processes. The above mentioned inherent characteristic of biomass leads to low process conversion efficiency, difficulties in grinding, collection, storage, and transportation [5,14]. In addition, application of biomass in co-pyrolysis with plastic, municipal solid waste and coal in thermal power plants for energy generation is increasing rapidly in recent time. Flow characteristics of biomass play an important role when it comes to blending biomass with other biomass, plastic materials during co-pyrolysis, and coal in co-firing process in thermal power plants. However, application of biomass in co-pyrolysis, combustion and co-firing is difficult to attain due difference in fuel and flow behavior of coal and biomass. Due to these drawbacks, at present, the global annual energy achieved from biomass is approximately 10% of the overall energy consumption [15,16]. It is therefore essential to improve the quality of biomass through pretreatment process and check the suitability of treated biomass in term of fuel and flow properties, before it can be used in thermochemical conversion process efficiently. In the past, various pretreatment methods have been explored to improve the quality of biomass. Among the various processes, torrefaction provides a promising route for the upgradation of biomass.

Torrefaction is defined as a mild pyrolysis process with the temperature zone of 200–300 °*C* at atmospheric pressure with inert medium at a low heating rate of (<20 °*C*/min) and residence time around 15–60 min [17–19]. Torrefaction takes place in four simple steps as discussed by van der Stelt et al. [15]**:** (a) Drying process through which mainly surface moisture is removed, (b) Post-drying through which bound moisture and some light hydrocarbons are removed, (c) Torrefaction process, which is mainly isothermal heating, on supplying heat depolymerization, partial devolatilization, and partial carbonization takes place, (d) Cooling process.

Many literatures are available that discuss the properties of torrefied biomass as good quality solid biofuel. From the literature it may be summarized that torrefied biomass has superior characteristics as comparison to raw biomass. The moisture content, oxygen content, hydrogen content, H/C and O/C ratio, and volatile matter decreased, while, fixed carbon content and higher heating value of raw biomass increased due to torrefaction [20,21]. The torrefied biomass has lesser moisture absorption capacity as compared to raw biomass which prevents its biological degradation and supports its long time storage as compared to raw biomass [22,23]. The destruction of fibrous and tenacious structure of biomass during torrefaction decreases its grinding energy requirement [24,25]. Thus, torrefied biomass as compared to raw biomass is well suited for thermochemical conversion processes such as combustion, pyrolysis and gasification. However, focus given on the study of fuel properties such as volatile ignitability (VI), combustibility index (CI), fuel ratio (FR) and flow properties such as Hausner ratio (HR), cohesion coefficient (C), Carr compressibility index (CCI) and angle of repose for raw and torrefied biomass and variation of these properties with process parameter during torrefaction is very less. Also, as per the knowledge of present authors, no work has been published about torrefaction of A*cacia nilotica* to check its suitability as good quality solid fuel.

Thus, torrefaction of *Acacia nilotica* was executed in a tubular reactor. To check the suitability of torrefied biomass as better quality solid biofuel or as a blend with coal, various tests have been performed. The fuel (volatile ignitability (VI), combustibility index (CI), fuel ratio (FR)), and flow (Hausner ratio (HR), cohesion coefficient (C), Carr compressibility index (CCI), angle of repose) properties, particle size, density, moisture sorption (open environment test and contact angle test) of torrefied biomass were analyzed. Also, the characteristics of torrefied biomass at different conditions were analyzed through TGA, FTIR, SEM-EDX and ICP-MS analysis. Finally, the characteristics of torrefied biomass were compared with properties of coal using published literature.

2. Experimental section

2.1. Materials

The wooden block of *Acacia nilotica*, about 1 ft in diameter was collected from village close to Banaras Hindu University (BHU) campus, Uttar Pradesh, India. The collected biomass was chopped into smaller with the help of an axe and further, fine particles between 0.7 and 1.25 mm were obtained after subsequent cutting (Cutting machine; Retsch model SM 300, Germany) and screening. The surface moisture of the biomass was removed by sun drying. After that biomass sample was again kept in an oven kept at 80 °*C* for overnight and then kept in air tight container prior to experiments.

2.2. Labelling of samples

In this study, the dried *Acacia nilotica* is denoted as DAN, and torrefied *Acacia nilotica* is denoted as TANX-Y, where the parameter X indicates the torrefaction temperature and Y denotes the residence time of the process. For example, TAN250-40 indicates torrefied *Acacia nilotica* which was obtained by torrefaction at 250 °*C* for 40 min.

2.3. Experimental setup and procedure for torrefaction

Fig. 1 depicts the setup used for experimental process. Table 1 represents the detail about the components of experimental setup and Table 2 denotes the list of controlled and measured variable during the experiments. The detailed procedure for experimental process can be found elsewhere [10]. All the

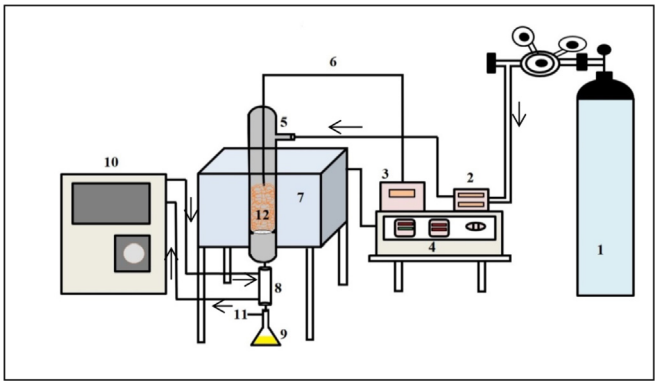

Fig. 1. Schematic diagram of experimental set-up: 1-nitrogen cylinder, 2-mass flow controller, 3-temperature measuring unit, 4- split tube furnace (NSW-104) controller, 5-long tube fixed bed reactor, 6-K-type thermocouple, 7- split tube furnace (NSW-104), 8-condenser, 9-oil collector, 10- chiller (Eyela CA-1112CE), 11-gas collector, 12-biomass with ceramic wool bed [10].

Table 1
Specifications/detail of instruments/variables used in experimental setup and procedure.

Variable/analysis	Instrument name/specification	Measurement Range	Uncertainty (%)
Temperature (°C)	K-type thermocouple	−270 to 1370 °C	±1.1 °C
Split tube furnace (NSW-104)	Single heating zone (length 455 mm) Microprocessed PID controller Work on 220 V AC 50 Hz	Max. 900 °C	
Heating rate (°C/min)	Set from control panel of furnace	–	±0.15 °C/min
Residence time (min)	Set from control panel of furnace	–	Nil
Nitrogen flow rate (mL/min)	Mass flow controller (Bronkhorst)	0–200 mL/min	±0.30% mL/min
Weighing machine	Sartorius weighing machine (BSA224S-CW)	Max. 250 g	±0.1 mg
Initial drying of sample	Laboratory Universal Hot air oven	Max. 260 °C	±5 °C
Proximate analysis	Muffle furnace	Max. 900 °C	±5 °C
Recirculating bath	Eyela CA-1112CE	−20 to 30 °C	±2 °C
Cutting machine	Retsch model SM 300	–	–

Table 2
List of controlled and measured variable during experiment.

Variable	Range/value
Controlled variable	
Heating rate (°C/min)	15
Sweeping gas flow rate (mL/min)	40
Particle size (mm)	0.7–1.25
Pressure	Atmospheric
Measured variable	
Temperature (°C)	220–280
Residence time (min)	20–60

experiments were performed twice to check the repeatability of results and average values have been reported.

The solid yield of biomass is calculated as:

$$Solid\ yield\ (SY) = \frac{m_{TAN}}{m_{DAN}} \quad (1)$$

where m_{TAN} is the mass of torrefied biomass at different process parameter and m_{DAN} is the mass of dried *Acacia nilotica*.

2.4. Physicochemical properties of raw and torrefied biomass

2.4.1. Proximate and ultimate analyses

Proximate analysis of biomass can be used to calculate moisture, volatile matter, fixed carbon, and ash content of the biomass sample. All these parameters were expressed on wet basis and dry basis and calculated using different ASTM standards mentioned in Table 3. The aim of ultimate analysis was to calculate the elemental composition (CHNS) of raw and torrefied biomass. The Element analyzer (EURO EA3000, EURO VECTOR instrument and software, ITALY) was used to execute ultimate analysis. Oxygen bomb calorimeter (Rajdhani Scientific, NSTTS Co., New Delhi, India) was employed to evaluate the heating value of raw biomass and torrefied biomass.

The energy density ratio and energy yield can be calculated using Eqs. (2) and (3):

Table 3
Different ASTM standards used to calculate engineering properties of torrefied biomass.

Physical parameter	ASTM standard used
Bulk density	ASTM E873-82
Moisture content	ASTM E871
Ash content	ASTM E1755
Volatile matter	ASTM E872
Heating value	ASTM D240
Angle of repose	ASTM C144

$$Energy\ density\ ratio\ (EDR) = \frac{HHV_{db,\ TAN}}{HHV_{db,\ DAN}} \quad (2)$$

$$Energy\ yield\ (EY) = SY \times EDR \quad (3)$$

The CHO index derived from the ultimate analysis of biomass to explain the oxidation state of carbon present in organic matter as recommended by Mann et al. [26]. It can be calculated as:

$$CHO\ index = \frac{2[O] - [H]}{[C]} \quad (4)$$

where [O], [H] and [C] are the mole fraction of oxygen, hydrogen, and carbon present in the organic material respectively.

2.4.2. Density, porosity, and particle size of raw and torrefied biomass

The density of biomass can be of three types: the bulk density, the tapped density, and the particle density. ASTM standard E873-82 is used to calculate the bulk density of biomass. The standard includes pouring the biomass sample into a standard-size container. In this study, a measuring cylinder of 500 mL is filled with biomass gently. The excess material over the cylinder was removed by a scale to level the biomass at the top of the measuring cylinder. The mass of the biomass present in the cylinder was weighed, and bulk density was calculated using the Eq. (5). The tapped bulk density of biomass can be calculated by tapping the cylinder containing the biomass until it reaches a constant volume (tap around 100 times). The tapped density (ρ_{Tb}) was calculated using Eq. (6). For calculation of particle density of biomass, it can be given a particular geometrical shape like cube, cuboid, sphere, and cylinder, etc. The mass of the shape and volume can be calculated, and division of both gives the particle density of biomass. The porosity of biomass sample can be defined as the pore spaces present in the bulk samples of biomass, and it can be calculated using the following Eq. (8).

$$\text{Bulk density},\ \rho_b(\text{kg/m}^3) = \frac{m_g - m_c}{V_L} \quad (5)$$

$$\text{Tapped density},\ \rho_{Tb}(\text{kg/m}^3) = \frac{m_t - m_c}{V_L} \quad (6)$$

$$\text{Particle density},\ \rho_p(\text{kg/m}^3) = \frac{m_p}{V_p} \quad (7)$$

$$\varepsilon_0 = 1 - \frac{\rho_b}{\rho_p} \tag{8}$$

where ρ_b is the bulk density, ρ_{Tb} is the tapped density, ρ_p is the density of particle, m_g is the total mass of cylinder and biomass (kg), m_c is the mass of empty cylinder (kg), m_t is the total mass of cylinder and biomass after tapping (kg), m_p is the mass of geometrical shape (kg) and V*p* is the volume of geometrical shape (m^3), V_L is the volume of measuring cylinder (m^3) and ε_0 is the porosity of biomass.

However, the biomass particle having irregular shape, the volume of particle can be calculated by deploying Eq. (9) given by Tooyserkani et al. [27].

$$Vp = Vc - V_R\left(\frac{P_1}{P_2} - 1\right) \tag{9}$$

where Vp is the volume of biomass (m^3), V_C is the sample cell volume (m^3), V_R is the reference volume (m^3), P_1 is the pressure after pressurizing the reference volume (Pa), and P_2 is the pressure after including V_C (Pa).

For particle size distribution, unsieved raw biomass obtained after grinding was torrefied at 220, 250, and 280 °*C*; then raw and torrefied biomass was sieved and analyzed. Both, raw and torrefied biomass were passed through a series of sieves having opening sizes (22, 25, 30, 36, 44, 52, 60 and 85 BSS) using a screen shaker. The sieves are arranged in the stack with largest opening at the top and smallest opening at the bottom. Size distribution for raw and torrefied biomass was analyzed by employing the procedure given by American National Standards Institute (ANSI). After completion of shaking process, biomass sample accumulated on every single screen has been weighed. Geometric mean diameter (d_{gm}) for raw and torrefied biomass was determined by employing the co-relation given by Cai et al. [28] in Eq. (10).

$$d_{gm} = log^{-1}\left(\frac{\sum M_i . log\sqrt{d_i . d_{i-1}}}{\sum M_i}\right) \tag{10}$$

where d_i is diagonal of screen apertures of ith screen, d_{i-1} is diagonal of the screen apertures in the next larger screen, and M_i is the mass retained on the ith screen.

2.4.3. Moisture sorption test of raw and torrefied biomass

2.4.3.1. Open environment test. In this work, the characteristics of raw biomass and torrefied biomass for moisture sorption were performed in an open environment (relative humidity 60%). For calculation of amount of moisture absorbed with respect to time, the sample DAN, TAN220-40, TAN250-40, and TAN280-40 were analyzed for the purpose. Weighed samples were kept for five days in an open environment. After estimated time, the samples were taken and weighed and percentage moisture absorbed was calculated using Eq. (11):

$$\%\ moisture\ absorbed = \frac{M_A - M_{Bi}}{M_A} \times 100 \quad i = 1\ to\ 5\ days \tag{11}$$

where M_A is the initial mass of the sample (kg), and M_{Bi} is the mass of sample after ith day (kg).

2.4.3.2. Contact angle measurement. To check the water absorption characteristics, water contact angle of raw and torrefied biomass were measured using contact angle analyzer (KRUSS, DSA25 Series, Hamburg, Germany). De-ionized water was used as a probe liquid. For contact angle measurement pellets from raw and torrefied biomass were made and contact angle was recorded using a sessile drop method at room temperature.

2.4.4. Flowability and combustion indices of raw and torrefied biomass

The flow characteristics of raw and torrefied biomass was investigated using Hausner ratio (HR), cohesion coefficient (C), Carr compressibility index (CCI) and angle of repose [29]. The angle of repose is defined as the steepest angle at which a stack of biomass particle can remain stable without slumping [30]. It may range from 0° to 90°. Different methods such as revolving cylinder method, tilting box method and fixed funnel method for analyzing the angle of repose have been described in literature [28,30]. However, in this study ASTM-C144 associated with fixed funnel method was employed to investigate angle of repose. In fixed funnel method (Fig. 2), the biomass particles obtained after sieving were poured very slowly through a funnel which was fixed through a stand at a certain height (H) from the base. The biomass coming out of funnel takes the shape of a cone. The pouring from the funnel was stopped when cone pile touched the lower tip of the funnel which was at a predetermined height (H). By measuring the radius of base of the cone, the angle of repose can be calculated using Eq. (12). Szalay et al. [31] derived a correlation for cohesion coefficient and concluded that cohesion coefficient depends on angle of repose and particle size of biomass. The cohesion coefficient was calculated by Eq. (13). HR and CCI vary with densities (bulk and tapped density) of biomass. HR and CCI of raw and torrefied biomass was obtained by employing Eqs. (14) and (15).

$$Angle\ of\ repose\ (\theta) = \tan^{-1}\left(\frac{H}{R}\right) \quad Where\ R = D/2 \tag{12}$$

$$Cohesion\ coefficient\ (C) = \frac{1}{2}d\left(\sqrt{cos^2\,\theta + \frac{4sin\theta}{d}} - cos\theta\right) \tag{13}$$

$$Hausner\ ratio\ (HR) = \frac{\rho_{Tb}}{\rho_b} \tag{14}$$

$$Carr\ compressibility\ index\ (CCI) = \left(1 - \frac{\rho_b}{\rho_{Tb}}\right) \times 100 \tag{15}$$

To evaluate the suitability of torrefied biomass as good quality solid bio-fuel, Conag et al. [32] mentioned combustion indices such as fuel ratio (FR), combustibility index (CI) and volatile ignitability

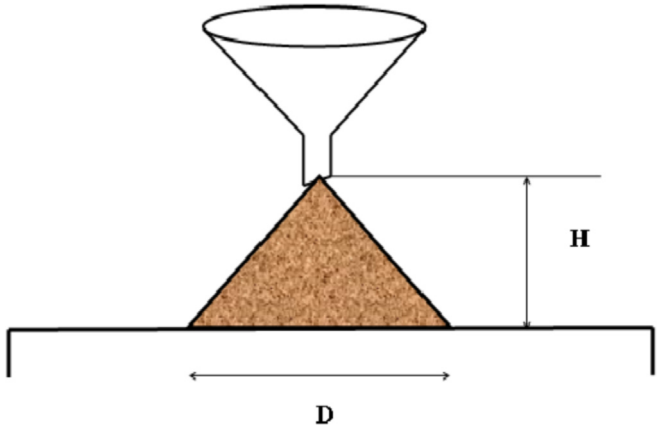

Fig. 2. Schematic diagram for calculation angle of repose.

(VI) and they were enumerated by using Eqs. (16) - (18).

$$Fuel\ ratio,\ FR = \frac{FC_{db}}{VM_{db}} \tag{16}$$

$$Combustibility\ index\ CI\ (MJ/kg) = \frac{HHV_{db}}{FR} \times (115 - Ashdb) \times \frac{1}{105} \tag{17}$$

$$Volatile\ ignitability,\ VI\ (MJ/kg) = \left[\frac{HHV_{db} - 0.338FC_{db}}{VM_{db} + M_{db}}\right] \times 100 \tag{18}$$

2.4.5. Analytical instruments used to characterize raw and torrefied biomass

Thermogravimetric analyzer (PerkinElmer STA 6000) was used to investigate the thermal behavior and mass loss characteristics. 5 mg of raw and torrefied biomass was heated from 25 to 800 °C in the presence of nitrogen atmosphere, at a flow rate of 20 mL/min and a constant heating rate of 5 °C/min. Fourier Transform Infrared Spectroscopy (FTIR) was done using (FTIR, Varian 1000, USA) for qualitative analysis of functional group present in raw and torrefied biomass after torrefaction. Oven dried Potassium Bromide (KBr) was used to make the pellets to reduce the interference from water. The spectra were recorded from 4000 to 400 cm^{-1} wavenumber. The surface morphology and elemental analysis of raw (DAN) and torrefied biomass (TAN220-40, TAN250-40, and TAN280-40) were studied by scanning electron microscopy (SEM, model JEOL JSM5410, Japan). Metal content present in raw and torrefied biomass was determined by using inductively coupled plasma-mass spectrometer (ICP-MS PerkinElmer Optima 7000 DV series). Sample were digested in nitric acid and diluted with double distilled water so that metal concentration falls into the detection limit.

3. Results and discussion

3.1. Solid product and energy yield of torrefied biomass

The outcomes of torrefaction process are torrefied biomass as solid product, condensable liquid and gaseous products. The amount of each product varies with operating conditions such as process temperature and residence time of biomass inside the reactor. Fig. 3 shows the variation of solid yield with temperature and residence time during torrefaction. When process temperature during torrefaction increases, the significant cleavage of hydroxyl group associated with biomass takes place. As a result, the amount of condensable liquid product with more water vapour increases with process temperature at fixed residence time. As an example, the solid yield was 61.82% and 43.03%, when the biomass was torrefied at 220 and 280 °C, respectively, at a constant residence time of 40 min. Hence, effectively, the solid yield decreased by 30.40% due to increase of process temperature at constant residence time. Moreover, solid yield also decreased with increase in residence time [33]. The solid yield decreased from 60.10% to 51.23%, when the residence time was increased from 20 to 60 min, at torrefaction temperature of 250 °C. It was observed that temperature had more pronounced effect than the residence time on torrefaction process. Subsequently, fuel and flow characteristics of torrefied biomass should also be more process temperature reliant than residence time. Keeping this in mind, all the properties of

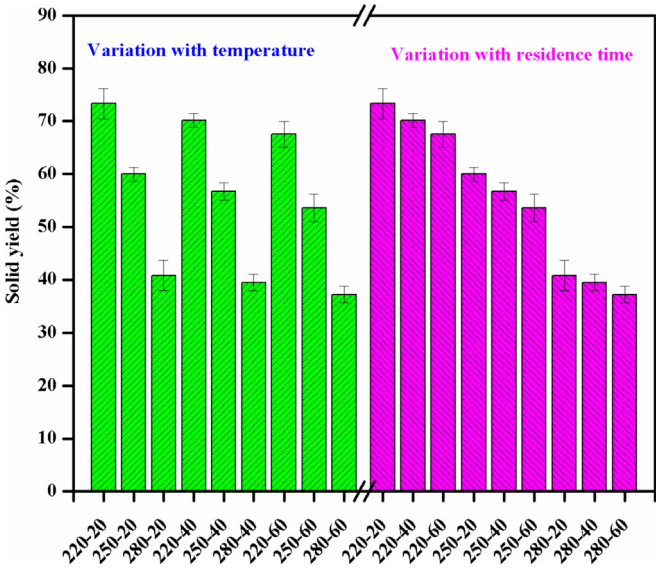

Fig. 3. Variation of solid yield with temperature and residence time.

torrefied biomass at three temperature (220, 250, and 280 °C) at 40 min residence time are calculated. The solid product yield from torrefaction often varies with biomass and its constituents. The biomass with higher fraction hemicellulose produces less solid product, as hemicellulose decomposition occurs at comparatively lower temperatures than cellulose and lignin [34,35]. The energy yield which is a product of solid yield and ratio of HHV of torrefied biomass to raw biomass indicates the amount of energy preserved in biomass after torrefaction. The energy yield of torrefied biomass (TAN220-40, TAN250-40, and TAN280-40) is found to be 74.10, 62.99, and 45.36%, respectively. It shows that with increase in temperature the energy yield decreases since at higher temperature, dehydrogenation and deoxygenation of biomass become more prominent.

The choice of optimum parameter for upgradation of raw biomass through torrefaction is based on the balance between higher heating value and energy yield of torrefied biomass. In this study, torrefaction at 250 °C, and residence time 40 is recommended since the energy yield of torrefied biomass is 62.99% and higher heating value is 22.54 MJ/kg.

3.2. Physicochemical characteristic of raw and torrefied products

The results from physicochemical analysis are presented in Table 4. It shows that both the moisture content and the volatile matter decreased with increase in temperature during process. The moisture content of biomass decreased from 6.18% (DAN) to 0.88% (TAN280-40). Besides, the volatile matter also decreased from 81.77% (DAN) to 36.84% (TAN280-40). Vassilev et al. [36] revealed that biomass having higher volatile matter is well suited for production of bio-oil through pyrolysis. The amount of volatile matter released from biomass depends on the temperature, residence time and heating rate during the process [28]. It should be mentioned that the quantity of bio-oil could be reduced if torrefied biomass (low volatile matter) is pyrolysed as compared to raw biomass (high volatile matter); however, the quality of bio-oil will be improved due to decreased O/C ratio as evident from Fig. 4. The ash content of biomass increased from 0.69% for DAN to 1.87% for TAN280-40. The fixed carbon increased from 11.35% for DAN to 60.40% for TAN280-40. The increase in fixed carbon and ash content of biomass was perceived after torrefaction since devolatilization of

Table 4
Proximate and ultimate analysis of raw and torrefied biomass.

Analysis	DAN	TAN220-40	TAN250-40	TAN280-40	Coal sample[#]
Proximate analysis (wt %)					
Moisture content	6.18	2.52	1.86	0.88	2.67
Ash content	0.69 (0.73)	1.24 (1.27)	1.39 (1.41)	1.87 (1.88)	6.63 (6.81)
Volatile matter	81.77 (87.15)	58.57 (60.08)	46.07 (46.94)	36.84 (37.16)	39.58 (40.66)
Fixed carbon[a]	11.35 (12.09)	36.66 (37.60)	50.66 (51.62)	60.40 (60.93)	51.12 (52.52)
Ultimate analysis (wt %)					
Carbon	43.84	50.31	58.62	64.75	76.48
Hydrogen	7.88	6.75	5.24	4.85	5.24
Nitrogen	0.42	0.63	0.69	0.64	2.32
Oxygen[a]	47.86	42.31	35.45	29.76	8.27
Sulphur	ND	ND	ND	ND	1.06
Higher heating value (MJ/kg)	19.31 (20.58)	20.77 (21.30)	22.54 (22.96)	24.76 (24.97)	30.42 (31.25)
Energy density ratio	–	1.19	1.11	1.05	–
Energy yield (%)	–	74.10	62.99	45.36	–

[a] Calculated by difference; ND Not detected; values in the parentheses are based on dry basis; # data for coal sample has been taken from Ref. [39].

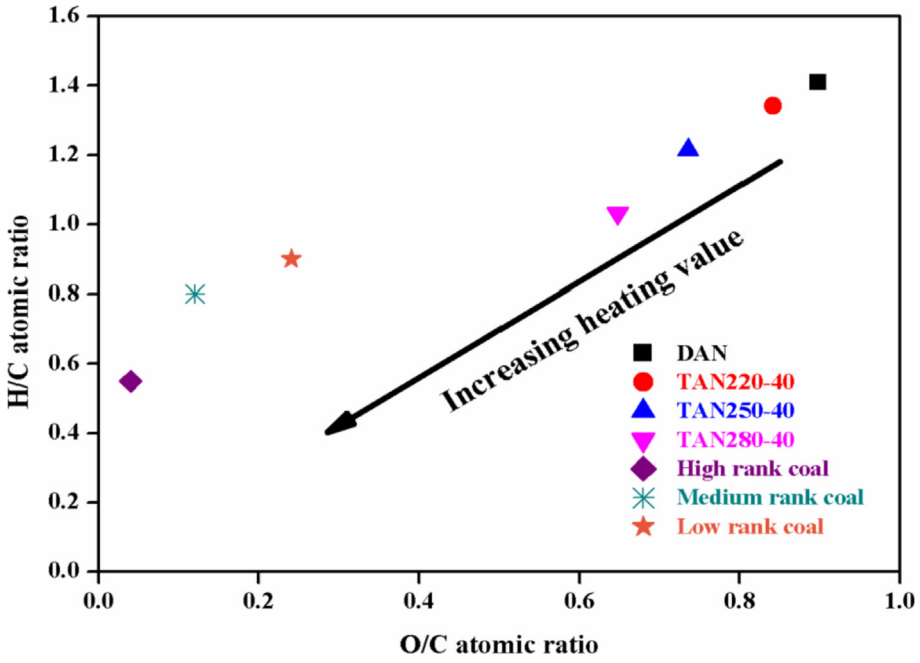

Fig. 4. Van Krevelen diagram for raw and torrefied biomass.

biomass increases with increase in temperature which results in relative decrease in moisture content and volatile matter and relative increase in fixed carbon and ash content of biomass. With increase in temperature, rate of release of light volatile matter (light hydrocarbon like methane, ethane, etc.) from biomass increases which affects the properties obtained from proximate analysis of biomass. During the torrefaction, release of hydrogen and oxygen in form of condensable liquid and gaseous products are more pronounced than release of carbon. The higher carbon content in biomass after torrefaction is accountable for increase in HHV of torrefied biomass. The higher heating values obtained for DAN, TAN220-40, TAN250-40, and TAN280-40 are 19.31, 20.77, 22.54, and 24.76 MJ/kg, respectively. Similar results for HHV were also obtained by Chen et al. [37], Chen et al. [38] and Phanphanich et al. [25] for same kind of biomass.

The van Krevelen diagram may be used to compare the elemental composition of biomass with that of coal. In this diagram, the atomic ratio of hydrogen to carbon (H/C) is plotted against the atomic ratio of oxygen to carbon (O/C). Fig. 4 shows the van Krevelen diagram for raw (DAN) and torrefied biomass (TAN220-40, TAN250-40, and TAN280-40). As the temperature increases during torrefaction, the amount of oxygen and hydrogen present in biomass decreased with the relative increase in carbon content. The carbon content of DAN and torrefied biomass (TAN220-40, TAN250-40, and TAN280-40) is found to be 43.84, 50.31, 58.62, and 64.75 wt%, respectively. Thus, with increase in temperature during torrefaction the carbon content of resulting solid product increases. The increase in carbon content of torrefied biomass is attributed to higher heating value of torrefied biomass. However, the solid yield decreases with increase in temperature (Fig. 3). Therefore, a balance between carbon content of torrefied biomass and solid product yield should be established. Hence, torrefaction at 250 °C and 40 min residence time is considered optimum for further studies. In addition, properties of torrefied biomass also move towards the properties of coal suggesting that torrefied biomass may be used as a substitute of coal. The ICP-MS was performed to analyze the effect of torrefaction on the metal content of raw biomass. The results are presented in Table 5. In can be observed that torrefied biomass is enriched in Sodium (Na), potassium (K), calcium (Ca), magnesium (Mg), iron (Fe), aluminum (Al), nickel (Ni)

Table 5
ICP-MS analysis of raw and torrefied biomass.

Elements	Concentration@ of elements in different sample				
	DAN	TAN220-40	TAN250-40	TAN280-40	Coal sample**
Na	219	238	316	387	209
K	29	45	88	142	974
Mg	107	122	176	284	252
Ca	642	880	1097	1864	1081
Al	27	32	73	155	6931
Fe	23	40	88	143	5591
Ni	3	4	4	8	9.8
Cr	ND	ND	ND	ND	11.7
Mn	2	2	3	5	12.3
Zn	ND	ND	ND	ND	12.5
Co	6	6	6	10	1.13
Be	ND	ND	ND	ND	0.52

@ Concentration of elements are presented in ppm; ND not detected; ** data for coal has been taken from Ref. [42].

and cobalt (Co) while some elements such as chromium, Zink, and beryllium were not detected. The concentration of detected elements increased with increase in temperature during torrefaction. Presence of elements in torrefied biomass might be responsible for higher reactivity of torrefied biomass than the raw biomass. Also, torrefied biomass may be used as an agent for soil amendment [40,41].

The range of CHO index can be from −4 to +4 [28]. Higher value of CHO index depicts more oxidized compounds, while lower CHO index depicts reduced molecules of oxidized compounds. The CHO index obtained for DAN, TAN220-40, TAN250-40, and TAN280-40 are −0.34, −0.34, −0.55 and −0.58, respectively. The typical value of CHO index for biomass varies between −0.50 and +0.05 [26,28]. This index decreases with increasing temperature of torrefaction and are presented in Table 6. This clearly shows that the oxygen content of biomass decreases during this process. A positive value of CHO index for any biomass suggests that the amount of oxygen present in biomass is quite high [26,28].

Color is an important parameter for biomass fuel, like the biomass having dark color, is known for its high ash content. The color of raw and torrefied biomass indicates the severity of process. The color of treated biomass has a direct relation with its calorific value, darker the treated biomass higher will be the calorific value. Fig. 5 shows the physical appearance of DAN, TAN220-40, TAN250-40, and TAN280-40. It can be clearly observed that torrefied biomass obtained at higher temperature had darker color and higher calorific value. In industries associated with biomass, color can be a time-saving parameter to judge the quality of biomass by preventing lab scale testing of properties like moisture content, calorific value and hydrophobicity. Tooyserkani et al. [27] suggested that pellets made from bark of wood were darker in color.

3.3. Density, porosity, and particle size raw and torrefied biomass

Three type of densities namely bulk, tapped and particle density and porosity of raw and torrefied biomass were calculated using equations (5)–(8). Density is a key physical parameter for crafting a system for storage, handling, and transport of biomass. Bulk density of biomass varies with moisture content, particle dimension (size and shape), and surface morphology [43,44]. The variation of density and porosity of raw and torrefied biomass obtained at different temperature is given Table 6. Results showed that densities (bulk, tapped and particle) of raw and torrefied biomass were reduced at higher process temperature, while, porosity of biomass increased due to removal of volatile content present in biomass. The porosity of raw biomass (DAN) and torrefied biomass at 280 °C (TAN280-40) were 0.79 and 0.83, respectively. These results are well supported by the results obtained by Conag et al. [32] for bulk and tapped density of biomass.

The dimensions (size and shape) of biomass particles have significant consequence on the mixing, fluidization, and surface area. It also affects the heat and mass transfer along with flow behavior of biomass particles. Hence, the thermochemical process involving various dimensions of biomass can have different efficiency and energy requirement. The particle size of biomass feedstocks highly affects the thermochemical conversion process. Generally biomass has irregular shape and size which creates difficulties in the precise measurement of dimension (length, width, and thickness). The precise description of biomass dimension is crucial for processing, handling, and storage. Sieve analysis is a major technique for characterization of particle size (geometric mean diameter) of raw and torrefied biomass. According to Eq. (10), the geometric mean diameters of DAN, TAN220-40, TAN250-40, and TAN280-40 are found to be 0.50, 0.48, 0.46 and 0.45 mm, respectively. The screen analysis of DAN, TAN220-40, TAN250-40, and TAN280-40 is shown in Fig. 6 (a) and (b). It was observed that at higher temperature

Table 6
Fuel and flow properties, different types of densities of raw and torrefied biomass.

Properties	DAN	TAN220-40	TAN250-40	TAN280-40	Coal sample
Fuel properties/indices[a]					
FR	0.13	0.62	1.09	1.63	1.29
CI (MJ/kg)	147.40	38.99	24.67	17.37	24.96
VI (MJ/kg)	15.76	15.69	15.65	15.37	31.15
H/C	0.17	0.13	0.08	0.07	0.06
O/C	1.09	0.84	0.60	0.45	0.10
VM/FC	7.20	1.59	0.90	0.60	0.77
CHO index	− 0.34	− 0.34	− 0.55	− 0.58	–
Flow properties[b]					
Angle of repose (°)	39.36	38.79	36.15	32.51	36.8
HR	1.29	1.27	1.21	1.18	1.10
CCI	22.85	21.44	17.35	15.86	9.23
C	0.40	0.39	0.36	0.33	0.28
Bulk density (kg/m^3)	230.82	210.34	190.18	172.84	727
Tapped density (kg/m^3)	299.21	267.77	230.13	205.43	801
Particle density (kg/m^3)	1220	1150	1110	1050	1500
Porosity	0.81	0.81	0.82	0.83	–
Particle size (mm)	0.50	0.48	0.46	0.45	–

[a] Data for fuel properties of coal has been taken from Ref. [39].
[b] Data for flow properties of coal has been taken from Ref. [45].

Fig. 5. Color appearance of raw and torrefied biomass.

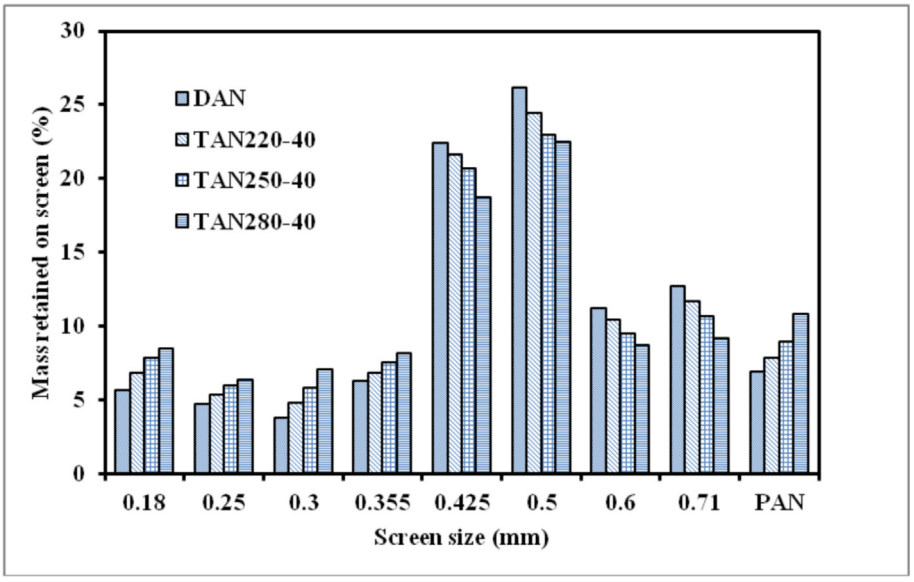

Fig. 6a. Particle size distribution of raw and torrefied biomass.

during torrefaction the fraction of smaller particle increases and uniformity in the particle size was obtained. Smaller particle obtained after torrefaction have lower heat resistance in further thermochemical process. Based on the results of screen analysis, SEM analysis, and density of torrefied biomass, it may be predicted that comminution of torrefied biomass becomes easier than the raw biomass. SEM analysis revealed that tenacious and fibrous structure of biomass is removed after torrefaction and pores were seen on the surface of biomass. Based on this observation, it may be noted that comminution of torrefied biomass is likely to be less energy-intensive process. In addition, decrease in density of biomass after torrefaction also favors easier comminution of torrefied biomass. Similar finding were reported by Arias et al. [46], and Tumuluru et al. [47]. Tumuluru et al. [47] optimized the grinding process using response surface methodology taking moisture content and grinder speed as input variables. They reported that at constant grinder speed of 20 Hz, specific grinding energy (kWh/ton) requirement would be lowered by 39.1% if the moisture content was reduced from 20 wt% to 10 wt %. In the present work the moisture content for TAN220-40, TAN250-40, and TAN280-40 was decreased by 59.22, 69.90, and 85.76%, respectively, as compare to the native biomass (DAN). Based on these observations, it can be mentioned that the comminution of torrefied biomass may be easier than that of raw biomass. Fig. 6 (b) shows the cumulative mass (wt%) retained on the screen and it was observed that mass of uniform particle size on each screen is

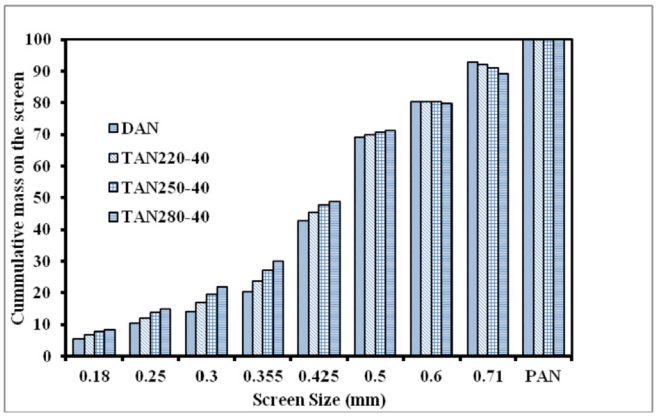

Fig. 6b. Cumulative mass distribution for raw and torrefied biomass.

obtained in case of torrefied biomass in contrast to raw biomass having unequal proportion of biomass on each screen. The larger biomass particle offers larger mass transfer and heat transfer resistance.

3.4. Moisture sorption characteristics of raw and torrefied biomass

The biomass has hydrophilic characteristics due to which it absorbs moisture when kept in open environment which causes biological degradation. Major constituents of biomass are hemicellulose, cellulose, and lignin. Each of these components contain hydroxyl group (-OH). Due to presence of this hydroxyl group biomass forms hydrogen bond with moisture, which makes it hygroscopic in nature. This higher moisture content in the biomass is undesirable since it leads to low energy efficiency, high energy loss, and higher emission when the biomass is used in thermochemical conversion process along with higher transport, storage and handling cost [35]. Fig. 7 (a) shows the percentage of moisture absorbed in raw biomass (DAN) and torrefied biomass (TAN220-40, TAN250-40, and TAN280-40). After five days, percentage of moisture absorbed by DAN, TAN220-40, TAN250-40, and TAN280-40 is 35.44%, 13.52%, 8.15% and 6.61% respectively. The torrefaction of biomass makes it hydrophobic in nature so that it absorbs minimal amount of moisture and becomes more stable when stored in an open environment.

During torrefaction, hydroxyl group (-OH) associated with biomass is ruptured resulting in lower affinity of biomass to associate with water through hydrogen bonding [35]. Torrefaction makes the biomass unsaturated which have non-polar properties. In addition, the tar present in the liquid condensate might get condensed on the surface and block the pores present in the torrefied biomass which can further reduce the water absorption capacity of torrefied biomass through capillary action [48]. This implies that the torrefaction can improve the logistic characteristics of biomass. The hydrophobic nature of torrefied biomass was also confirmed by contact angle measurement. For hydrophobic character the value of contact angle should be close to 90° [33]. Fig. 7 (b) shows the contact angle of raw and torrefied biomass. The contact angle from left and right side of the meniscus for DAN, TAN220-40, TAN250-40, and TAN280-40 was found to be 46.5–47.8°, 64.9–64.3°, 70.3–70.1° and 79.9–77.5° respectively. Thus, it can be concluded that hydrophobic characteristics of biomass increases with increase in temperature during torrefaction.

3.5. Flowability of raw and torrefied biomass

Flowability is the property of biomass which depicts the ease of motion of biomass from one point to other during the process. The flowability is an important characteristic of biomass which plays a crucial role during its utilization in conversion and co-conversion processes. The flow characteristics of raw and torrefied biomass are shown in Table 6. The flow behavior of raw and torrefied biomass based on Hausner ratio (HR), cohesion coefficient (C), Carr compressibility index (CCI) and angle of repose were analyzed and compared from Table 7 obtained from literature. The angle of repose for DAN, TAN220-40, TAN250-40, and TAN280-40 are 39.36, 38.79, 36.15, and 32.51 respectively. The calculated value of Hausner ration in this work for DAN, TAN220-40, TAN250-40, and TAN280-40 are 1.29, 1.27, 1.21 and 1.18, respectively, while, Carr compressibility index of DAN, TAN220-40, TAN250-40, and TAN280-40 are 22.85, 21.44, 17.35 and 15.86, respectively. The cohesion coefficient of DAN, TAN220-40, TAN250-40, and TAN280-40 are 0.40, 0.39, 0.36, and 0.33, respectively. During the course of torrefaction, solid product obtained at higher temperature has lower angle of repose and has better flowing property than the raw biomass.

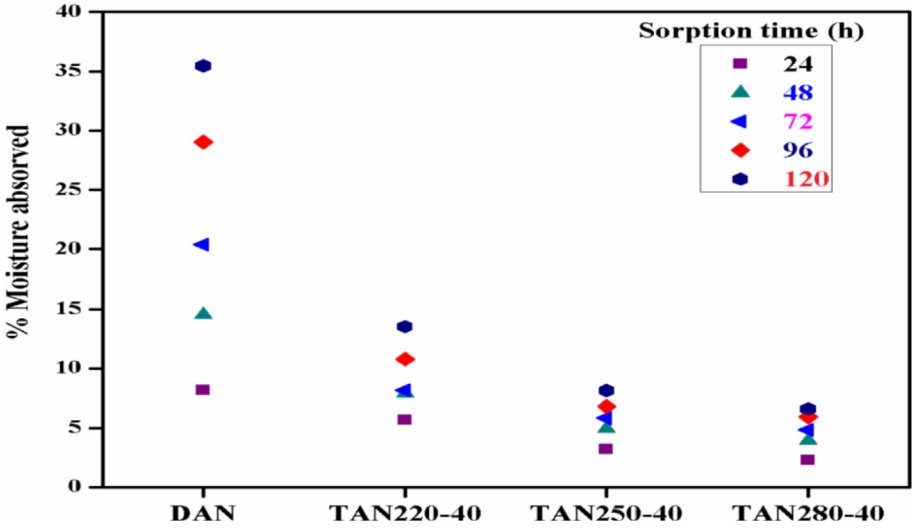

Fig. 7a. Moisture sorption test of raw and torrefied biomass in open environment.

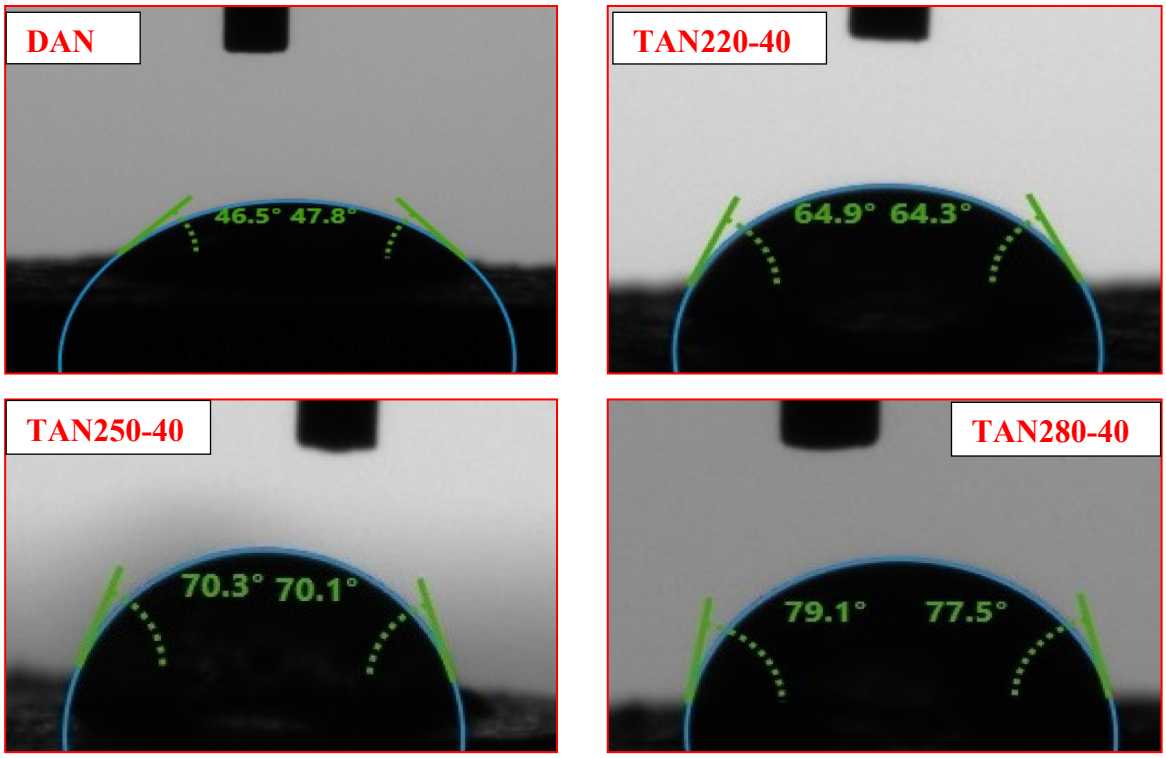

Fig. 7b. Moisture sorption test of raw and torrefied biomass using contact angle measurement.

Table 7
Characteristic flow properties of biomass [29,31].

Flow property	Angle of repose (degree)	Hausner ratio (HR)	Carr compressibility index (CCI)
Excellent	25–30	1.00–1.11	
Good	31–35	1.12–1.18	11–15
Fair	36–40	1.19–1.25	16–20
Passable	41–45	1.26–1.34	21–25
Poor	46–55	1.35–1.45	26–31
Very Poor	56–65	1.46–1.59	32–37
Very very Poor	>66	>1.60	> 38

The biomass torrefied at a higher temperature has better flowing property than raw or low temperature torrefied material. The Carr compressibility index of DAN, TAN220-40, TAN250-40, and TAN280-40 are 22.85, 21.44, 17.35 and 15.86 respectively. The torrefied biomass at higher temperature has lower tendency to agglomerate resulting in better flow behavior in comparison to raw biomass. Cohesion coefficient signifies the cohesive and frictional force of biomass particles [31]. The cohesion coefficient of DAN, TAN220-40, TAN250-40, and TAN280-40 are 0.40, 0.39, 0.36, and 0.33, respectively, which revealed that cohesive force in case of torrefied biomass is lower than the raw biomass resulting in better flow behavior of torrefied biomass as compared to raw biomass.

3.6. Combustion indices of raw and torrefied biomass

Table 6 presents the combustion indices of raw and torrefied biomass. The combustion indices are generally used to define quality of torrefied biomass after thermochemical conversion processes. Fuel ratio (FR), combustibility index (CI), and volatile ignitability (VI) are determined using equations (16)–(18), respectively. The fuel ratio of raw biomass increased after torrefaction due to increase in fixed carbon and simultaneous decrease in volatile content of biomass. In case of coal, the recommended range for fuel ratio is 0.5–3.0. The torrefied biomass obtained at 280 °C and 40 min residence time having the fuel ratio 1.63 which makes it suitable for firing in power plants along with coal. The higher fuel ratio causes an incomplete burning of fuel which reduces the efficiency of boiler when such fuel is used during its operation. During the process, the fuel with a fuel ratio greater than two may cause problems with ignition and flammability. The published combustibility index and volatile ignitability ranges are: combustibility index should be below 23 MJ/kg and volatile ignitability should be above 14.5 MJ/kg [48]. The value of combustibility index and volatile ignitability of raw *Acacia nilotica* (DAN) are 147.40 MJ/kg and 15.76 MJ/kg, respectively. It means that, without prior treatment raw biomass cannot be suited as an alternative energy source. The calculated value of combustibility index for TAN220-40, TAN250-40, and TAN280-40 are 38.99, 24.67, and 17.37 MJ/kg, respectively. The calculated value of VI for TAN220-40, TAN250-40, and TAN280-40 are 15.69, 15.65, and 15.37 MJ/kg, individually. Similar kind results were obtained by Singh et al. [21]. It shows that torrefied biomass obtained at 280 °C has nearly comparable characteristics like coal, and it can be used as a substitute source of energy and also, torrefied biomass can be blended with coal.

3.7. Thermogravimetric analysis

Fig. 8 (a) shows the thermogravimetric analysis of raw and torrefied biomass. The plot revealed that, in case of torrefied biomass, fixed amount decomposition attained at higher temperature. For DAN, mass loss of 20% was attained at 280 °C, however, the same amount of mass loss was observed at 336, 351, and 496 °C in case of TAN220-40, TAN250-40, and TAN280-40, respectively. This shifting of decomposition temperature for torrefied biomass might be due to breakdown of hemicellulose and retaining most of the cellulose and lignin. The different components of biomass have range of temperature for thermal decomposition. Hemicellulose and cellulose, generally decomposed at between 200 and 350 °C, while lignin decomposed between 280 and 600 °C [49]. For hemicellulose and cellulose, substantial weight loss was observed from 268 °C to 355 °C [14]. The DTG curve of raw and torrefied biomass are presented in Fig. 8 (b). At around 300 °C, a shoulder in DTG curve of biomass corresponds to degradation of hemicellulose [14,50]. In present work similar kind of shoulder is appeared in case of raw biomass Fig. 8 (b). However, in case of torrefied biomass (TAN220-40, TAN250-40 and TAN280-40), the shoulder cannot be observed, which revealed that the hemicellulose of raw biomass has decomposed in course of torrefaction. In DTG curve, the peak associated with maximum mass loss corresponds to cellulose content of biomass [14]. Around 340 °C, similar peaks attributed to cellulose can be perceived in case of raw and torrefied biomass which signifies lesser decomposition of cellulose in comparison to hemicellulose during torrefaction. However, intensity of peak for torrefied biomass decreases as the temperature increases during the process.

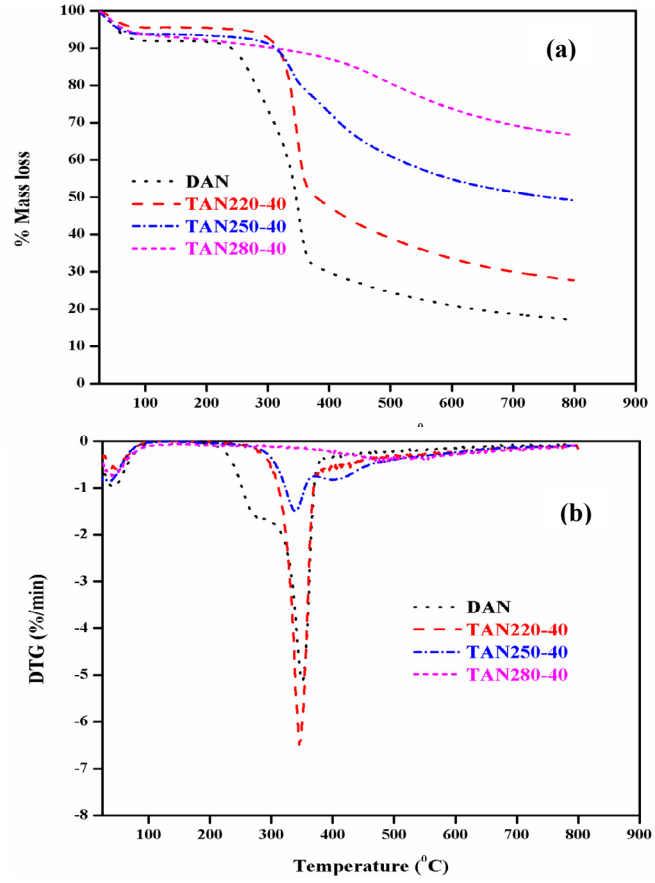

Fig. 8. Thermogravimetric analysis of raw and torrefied biomass (a) TGA analysis (b) DTG analysis.

3.8. FTIR analysis of raw and torrefied biomass

The analysis of various chemical functional groups present in raw biomass and corresponding changes in then after torrefaction was analyzed by employing Fourier transform infrared spectroscopy (FTIR). The breakdown of hemicellulose during torrefaction is mainly accountable for alteration in chemical structure of raw biomass. The distinctive peak among 3300-3100 cm^{-1} ascribed the stretching vibration of hydroxyl group (-OH) associated with hemicellulose of biomass. It also confirmed the hydrogen bond present between alcohol and phenol groups associated with hemicellulose and cellulose component of biomass [51]. Decrease in intensity from 3300 to 3100 cm^{-1} waveband inferred the breaking of hydrogen bond present between alcohol and phenol. This increases the durability of biomass against the moisture and biological attacks along with make it suitable for long storage, easy handling, and transportation (See. Fig. 9).

The specific peaks between 2900 and 2750 cm^{-1}, 1750-1500 cm^{-1}, and 1200-1000 cm^{-1} were observed due to stretching vibration in C═O bond, C═C bond, C–H bond, and C–O–C bond respectively [52–54]. With increase in temperature during torrefaction, the in intensity of peaks reaffirming the rupture of chemical bonds such as C═O, C–O–C, CHO- etc. present in the biomass. Reduction in peak intensity from 1750 to 1500 cm^{-1} corresponds to cleavage of ester group associated with hemicellulose through deacetylation reaction [55]. The characteristic peak between wavenumber 600-700 cm^{-1}, attributed to existence of aromatic compounds with mono and cyclic groups [56].

3.9. SEM-EDX analysis of raw and torrefied biomass

The scanning electron microscopy (SEM) analysis of raw biomass (DAN) and torrefied biomass (TAN220-40, TAN250-40 and TAN280-40) at 2K magnification are depicted in Fig. 10 to investigate the impact of torrefaction on biomass morphology. The effect of torrefaction could be clearly perceived in Fig. 10 (c), (e), and (g). Hemicelluloses are typically branched polysaccharides comprising solid bulky and branched xylem tissues [22]. Hemicellulose is elucidated by a branched arrangement associated with the raw biomass. Nevertheless, in the case of torrefied biomass, this branched structure began to disappear, indicating hemicellulose degradation during torrefaction (Fig. 10 (c), (e), and (g)). The formation of pores is visible for TAN220-40, TAN250-40, and TAN280-40. An increase in the pore size with increasing temperature could be seen from Fig. 10 (g) where the biomass was torrefied at 280 °C

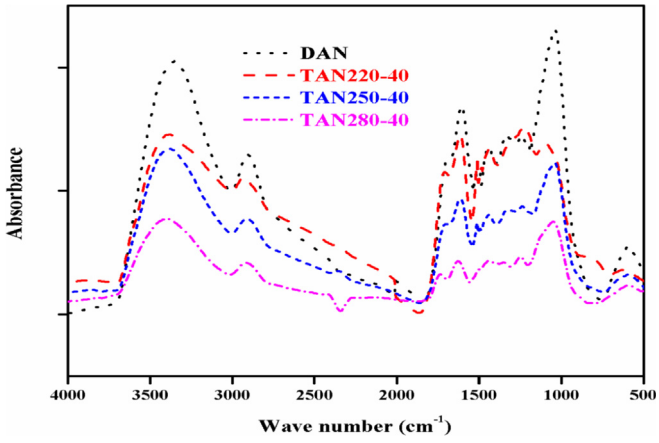

Fig. 9. FTIR analysis of raw and torrefied biomass.

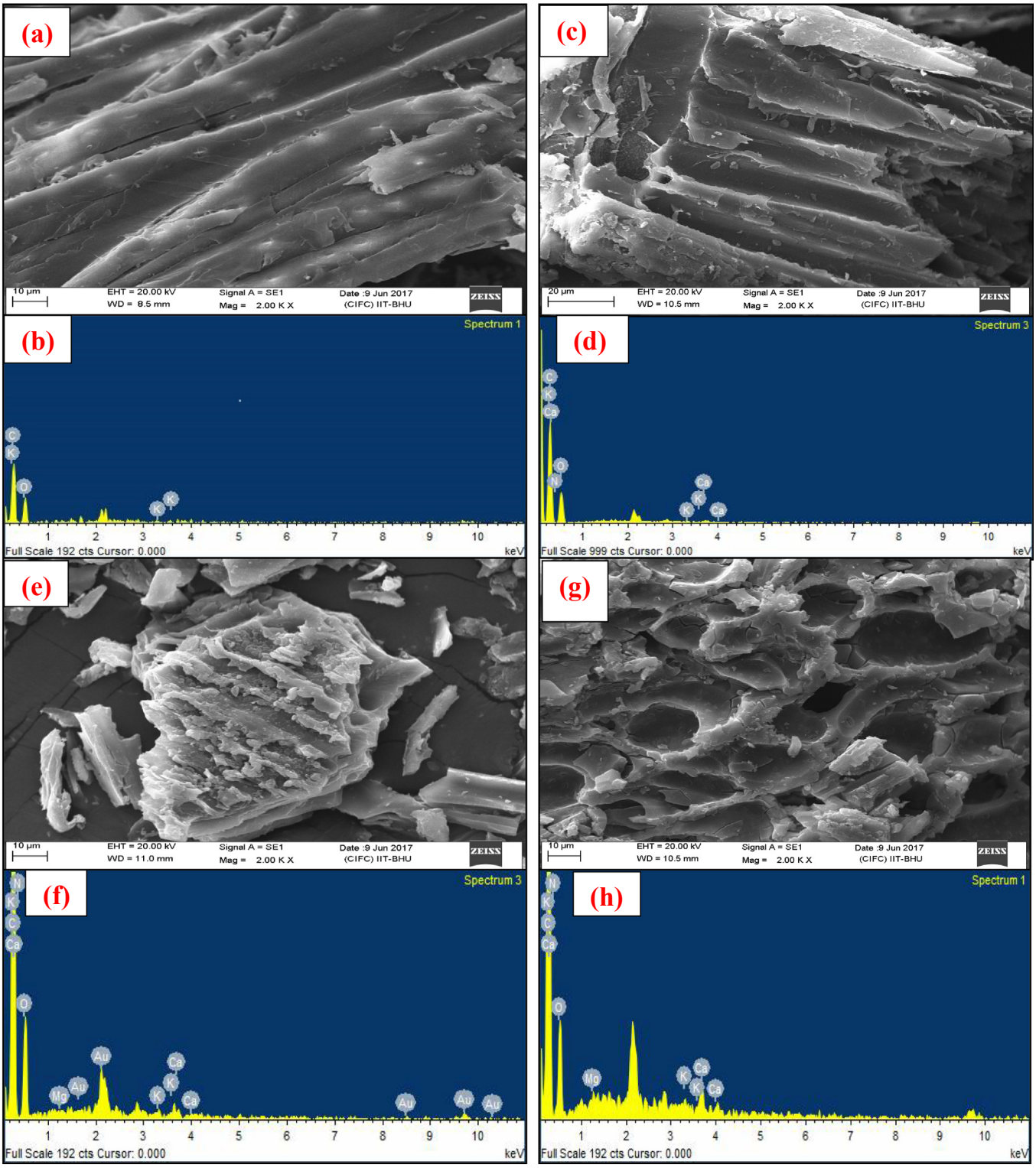

Fig. 10. SEM and EDX images of raw and torrefied biomass: (a) and (b) DAN, (c) and (d) TAN220-40, (e) and (f) TAN250-40 and (g) and (h) TAN280-40.

for 40 min. The appearance of pores on the surface of torrefied biomass was ascribed its lower density than the raw biomass which can increase the surface area and lower grinding energy as compared to raw biomass. Ibrahim et al. [22], and Bach et al. [35] mentioned the similar kind of results. Along with SEM analysis, energy dispersive X-ray (EDX) was also performed to identify elements present on the surface of raw and torrefied biomass. EDX images of raw (DAN) and torrefied biomass (TAN220-40, TAN250-40, and TAN280-40) are depicted in Fig. 10 (b) (d) (f) and (h), respectively.

The results revealed that with increase in severity of the torrefaction process, peaks corresponding to nitrogen, calcium, magnesium and potassium are appearing in torrefied biomass (TAN220-40, TAN250-40, and TAN280-40) with high intensity.

However, in case of raw biomass, only carbon, oxygen and potassium can be seen. Presence of these elements in the torrefied biomass makes it suitable for soil amendment to increase the fertility of soil [40,41].

4. Conclusions

Experimental investigation of torrefaction of *Acacia nilotica* within a temperature range of 220–280 °C and residence time between 20 and 60 min was performed. Various properties which validate good quality of solid fuel from biomass were examined. Results showed that temperature during torrefaction had more pronounced effect on solid yield as compared to residence time. Fuel and flow characteristics of *Acacia nilotica* has been improved after torrefaction and are closure to the properties of coal. The higher heating value (HHV) increased by 28.2% when raw biomass was torrefied at 280 °C for 40 min. Torrefied *Acacia nilotica* was found to be less hygroscopic as moisture reabsorbed was 6.61% (TAN280-40, 120 h) as compared to 35.44% (DAN, 120 h). Also, the contact angle of TAN280-40 (79.1°/77.5°) was close to 90° confirming the hydrophobic nature. The bulk density of torrefied DAN was suitable for use as briquette and co-firing with coal in thermal plants with HR value less than 1.29 and CCI less than about 23. There was significant decrease in volatile matter (57.4%) with simultaneous increase in fixed carbon content (~4 times). Hence, less volatile matter and high fixed carbon make torrefied *Acacia nilotica* a better solid fuel. TGA results showed that devolatilization temperature shifted to higher value and residual char yield increases when torrefied *Acacia nilotica* was pyrolysed. ICP-MS analysis revealed that torrefied biomass enriched by important elements such as sodium (Na), potassium (K), calcium (Ca), magnesium (Mg) etc. making it suitable for soil amendment. Finally, *Acacia nilotica* exhibited better performance as compared to other woody biomass because of enhanced HHV, low ash content etc.

Declaration of competing interest

The authors declare that they have no known competing financial interests or personal relationships that could have appeared to influence the work reported in this paper.

CRediT authorship contribution statement

Satyansh Singh: Writing - original draft. **Jyoti Prasad Chakraborty:** Funding acquisition, Project administration. **Monoj Kumar Mondal:** Writing - review & editing.

Acknowledgement

The authors acknowledge the funding from Science and Engineering Research Board (SERB), New Delhi, Indian through fund no. SR/FTP/ETA-56/2012. Authors are also grateful to the department of chemical engineering and technology and Central Instrument Facility Centre (CIFC), Indian Institute of Technology, (BHU) Varanasi, for conducting the work.

References

[1] X. Song, Y. Yang, M. Zhang, K. Zhang, D. Wang, Ultrasonic pelleting of torrefied lignocellulosic biomass for bioenergy production, Renew. Energy 129 (2018) 56–62.
[2] D. Magalhães, A. Panahi, F. Kazanç, Y.A. Levendis, Comparison of single particle combustion behaviours of raw and torrefied biomass with Turkish lignites, Fuel 241 (2019) 1085–1094.
[3] Y. Yue, H. Singh, B. Singh, S. Mani, Torrefaction of sorghum biomass to improve fuel properties, Bioresour. Technol. 232 (2017) 372–379.
[4] Y. Yang, M. Sun, M. Zhang, K. Zhang, D. Wang, C. Lei, A fundamental research on synchronized torrefaction and pelleting of biomass, Renew. Energy 142 (2019) 668–676.
[5] P. Giudicianni, G. Cardone, R. Ragucci, Cellulose, hemicellulose and lignin slow steam pyrolysis: thermal decomposition of biomass components mixtures, J. Anal. Appl. Pyrolysis 100 (2013) 213–222.
[6] K. Bargali, S. Bargali, Acacia nilotica: a multipurpose leguminous plant, Nat. Sci. 7 (2009).
[7] D. Raj, V. Haokip, S. Chandrawanshi, Acacia nilotica:A multipurpose tree and source of Indian gum Arabic, South Ind. J. Bio Sci. 1 (2015) 66–69.
[8] R.G. Saratale, G.D. Saratale, S.-K. Cho, G. Ghodake, A. Kadam, S. Kumar, Phytofabrication of silver nanoparticles by Acacia nilotica leaves: investigating their antineoplastic, free radical scavenging potential and application in H_2O_2 sensing, J. Taiwan Inst. Chem. Eng. 99 (2019) 239–249.
[9] C. Pandey, D. Sharma, Ecology of Acacia nilotica–based traditional agroforestry system in central India, Bull. NIE 15 (2005) 109–116.
[10] S. Singh, J. Prasad Chakraborty, M. Kumar Mondal, Intrinsic kinetics, thermodynamic parameters and reaction mechanism of non-isothermal degradation of torrefied Acacia nilotica using isoconversional methods, Fuel 259 (2020) 116263.
[11] S. Singh, J.P. Chakraborty, M.K. Mondal, Optimization of process parameters for torrefaction of Acacia nilotica using response surface methodology and characteristics of torrefied biomass as upgraded fuel, Energy 186 (2019) 115865.
[12] T.B. Gupta, D.H. Lataye, Removal of crystal violet and methylene blue dyes using Acacia Nilotica sawdust activated carbon, IJCT 26 (1) (2019) 52–68.
[13] R. Garg, N. Anand, D. Kumar, Pyrolysis of babool seeds (Acacia nilotica) in a fixed bed reactor and bio-oil characterization, Renew. Energy 96 (2016) 167–171.
[14] H. Yang, R. Yan, H. Chen, D.H. Lee, C. Zheng, Characteristics of hemicellulose, cellulose and lignin pyrolysis, Fuel 86 (12) (2007) 1781–1788.
[15] M.J.C. van der Stelt, H. Gerhauser, J.H.A. Kiel, K.J. Ptasinski, Biomass upgrading by torrefaction for the production of biofuels: a review, Biomass Bioenergy 35 (9) (2011) 3748–3762.
[16] W.-H. Chen, P.-C. Kuo, A study on torrefaction of various biomass materials and its impact on lignocellulosic structure simulated by a thermogravimetry, Energy 35 (6) (2010) 2580–2586.
[17] O. Kutlu, G. Kocar, Upgrading lignocellulosic waste to fuel by torrefaction: characterisation and process optimization by response surface methodology, Int. J. Energy Res. 42 (15) (2018) 4746–4760.
[18] M. Manouchehrinejad, Y. Yue, R.A.L. de Morais, L.M.O. Souza, H. Singh, S. Mani, Densification of thermally treated energy cane and napier grass, Bio Energy Res. 11 (3) (2018) 538–550.
[19] B. Keivani, S. Gultekin, H. Olgun, A.T. Atimtay, Torrefaction of pine wood in a continuous system and optimization of torrefaction conditions, Int. J. Energy Res. 42 (15) (2018) 4597–4609.
[20] J. Hu, B. Jiang, J. Wang, Y. Qiao, T. Zuo, Y. Sun, Physicochemical characteristics and pyrolysis performance of corn stalk torrefied in aqueous ammonia by microwave heating, Bioresour. Technol. 274 (2019) 83–88.
[21] Rk Singh, A. Sarkar, J.P. Chakraborty, Effect of torrefaction on the physicochemical properties of pigeon pea stalk (Cajanus cajan) and estimation of kinetic parameters, Renew. Energy 138 (2019) 805–819.
[22] R.H.H. Ibrahim, L.I. Darvell, J.M. Jones, A. Williams, Physicochemical characterisation of torrefied biomass, J. Anal. Appl. Pyrolysis 103 (2013) 21–30.
[23] S. Kanwal, N. Chaudhry, S. Munir, H. Sana, Effect of torrefaction conditions on the physicochemical characterization of agricultural waste (sugarcane bagasse), Waste Manag. 88 (2019) 280–290.
[24] M. Manouchehrinejad, I. van Giesen, S. Mani, Grindability of torrefied wood chips and wood pellets, Fuel Process. Technol. 182 (2018) 45–55.
[25] M. Phanphanich, S. Mani, Impact of torrefaction on the grindability and fuel characteristics of forest biomass, Bioresour. Technol. 102 (2) (2011) 1246–1253.
[26] B.F. Mann, H. Chen, E.M. Herndon, R.K. Chu, N. Tolic, E.F. Portier, Indexing permafrost soil organic matter degradation using high-resolution mass spectrometry, PloS One 10 (6) (2015) 1–16.
[27] Z. Tooyserkani, S. Sokhansanj, X. Bi, J. Lim, A. Lau, J. Saddler, Steam treatment of four softwood species and bark to produce torrefied wood, Appl. Energy 103 (2013) 514–521.
[28] J. Cai, Y. He, X. Yu, S.W. Banks, Y. Yang, X. Zhang, Review of physicochemical properties and analytical characterization of lignocellulosic biomass, Renew. Sustain. Energy Rev. 76 (2017) 309–322.
[29] G. Lumay, F. Boschini, K. Traina, S. Bontempi, J.C. Remy, R. Cloots, Measuring the flowing properties of powders and grains, Powder Technol. 224 (2012) 19–27.
[30] Rous, P. eacute, Comparison of methods for the measurement of the angle of repose of granular materials, Geotech Test. J. 37 (2014) 164–168.
[31] A. Szalay, A. Kelemen, K. Pintye-Hódi, The influence of the cohesion coefficient (C) on the flowability of different sorbitol types, Chem. Eng. Res. Des. 93 (2015) 349–354.
[32] A.T. Conag, J.E.R. Villahermosa, L.K. Cabatingan, A.W. Go, Energy densification of sugarcane bagasse through torrefaction under minimized oxidative atmosphere, J. Environ. Chem. Eng. 5 (6) (2017) 5411–5419.
[33] M. Strandberg, I. Olofsson, L. Pommer, S. Wiklund-Lindström, K. Åberg, A. Nordin, Effects of temperature and residence time on continuous torrefaction of spruce wood, Fuel Process. Technol. 134 (2015) 387–398.
[34] D.A. Granados, F. Chejne, P. Basu, A two dimensional model for torrefaction of

large biomass particles, J. Anal. Appl. Pyrolysis 120 (2016) 1–14.
[35] Q.-V. Bach, Ø. Skreiberg, Upgrading biomass fuels via wet torrefaction: a review and comparison with dry torrefaction, Renew. Sustain. Energy Rev. 54 (2016) 665–677.
[36] S.V. Vassilev, D. Baxter, L.K. Andersen, C.G. Vassileva, An overview of the composition and application of biomass ash. Part 1. Phase–mineral and chemical composition and classification, Fuel 105 (2013) 40–76.
[37] W.-H. Chen, J. Peng, X.T. Bi, A state-of-the-art review of biomass torrefaction, densification and applications, Renew. Sustain. Energy Rev. 44 (2015) 847–866.
[38] Q. Chen, J. Zhou, B. Liu, Q. Mei, Z. Luo, Influence of torrefaction pretreatment on biomass gasification technology, Chin. Sci. Bull. 56 (14) (2011) 1449–1456.
[39] S. Shabbar, I. Janajreh, Thermodynamic equilibrium analysis of coal gasification using Gibbs energy minimization method, Energy Convers. Manag. 65 (2013) 755–763.
[40] G.K. Gupta, M. Ram, R. Bala, M. Kapur, M.K. Mondal, Pyrolysis of chemically treated corncob for biochar production and its application in Cr(VI) removal, Environ. Prog. Sustain. Energy 37 (5) (2018) 1606–1617.
[41] C.A. Mullen, A.A. Boateng, N.M. Goldberg, I.M. Lima, D.A. Laird, K.B. Hicks, Bio-oil and bio-char production from corn cobs and stover by fast pyrolysis, Biomass Bioenergy 34 (1) (2010) 67–74.
[42] M.V. Balarama Krishna, K. Chandrasekaran, S. Chakravarthy, D. Karunasagar, An integrated approach based on oxidative pyrolysis and microwave-assisted digestion for the multi-elemental analysis of coal samples by ICP-based techniques, Fuel 158 (2015) 770–778.
[43] S.V. Bhagwanrao, M. Singaravelu, Bulk density of biomass and particle density of their briquettes, Int. J. Agric. Eng. 7 (2014) 221–224.
[44] P.S. Lam, S. Sokhansanj, X. Bi, J. Lim C, L.J. Naimi, M. Hoque, Bulk density of wet and dry wheat straw and switchgrass particles, Appl. Eng. Agric. 24 (3) (2008) 351.
[45] H. Lu, X. Guo, Y. Liu, X. Gong, Effect of particle size on flow mode and flow characteristics of pulverized coal, KONA Powder Par. J. 32 (2015) 143–153.
[46] B. Arias, C. Pevida, J. Fermoso, M.G. Plaza, F. Rubiera, J.J. Pis, Influence of torrefaction on the grindability and reactivity of woody biomass, Fuel Process. Technol. 89 (2) (2008) 169–175.
[47] J.S. Tumuluru, D.J. Heikkila, Biomass grinding process optimization using response surface methodology and a hybrid genetic algorithm, Bioengineering 6 (1) (2019) 12.
[48] T.-I. Ohm, J.-S. Chae, J.-K. Kim, S.-C. Oh, Study on the characteristics of biomass for co-combustion in coal power plant, J. Mater. Cycles Waste Manag. 17 (2) (2015) 249–257.
[49] S. Ren, H. Lei, L. Wang, Q. Bu, S. Chen, J. Wu, Thermal behaviour and kinetic study for woody biomass torrefaction and torrefied biomass pyrolysis by TGA, Biosyst. Eng. 116 (4) (2013) 420–426.
[50] M. Müller-Hagedorn, H. Bockhorn, L. Krebs, U. Müller, A comparative kinetic study on the pyrolysis of three different wood species, J. Anal. Appl. Pyrolysis 68–69 (2003) 231–249.
[51] F. Min, M. Zhang, Y. Zhang, Y. Cao, W.-P. Pan, An experimental investigation into the gasification reactivity and structure of agricultural waste chars, J. Anal. Appl. Pyrolysis 92 (1) (2011) 250–257.
[52] M. Keiluweit, P.S. Nico, M.G. Johnson, M. Kleber, Dynamic molecular structure of plant biomass-derived black carbon (biochar), Environ. Sci. Technol. 44 (4) (2010) 1247–1253.
[53] R.K. Sharma, J.B. Wooten, V.L. Baliga, M.R. Hajaligol, Characterization of chars from biomass-derived materials: pectin chars, Fuel 80 (12) (2001) 1825–1836.
[54] R. Azargohar, S. Nanda, J.A. Kozinski, A.K. Dalai, R. Sutarto, Effects of temperature on the physicochemical characteristics of fast pyrolysis bio-chars derived from Canadian waste biomass, Fuel 125 (2014) 90–100.
[55] F. Carrasco, C. Roy, Kinetic study of dilute-acid prehydrolysis of xylan-containing biomass, Wood Sci. Technol. 26 (3) (1992) 189–208.
[56] V. Gomez-Serrano, J. Pastor-Villegas, A. Perez-Florindo, C. Duran-Valle, C. Valenzuela-Calahorro, FT-IR study of rockrose and of char and activated carbon, J. Anal. Appl. Pyrolysis 36 (1) (1996) 71–80.